

# RSC Advances



This is an *Accepted Manuscript*, which has been through the Royal Society of Chemistry peer review process and has been accepted for publication.

*Accepted Manuscripts* are published online shortly after acceptance, before technical editing, formatting and proof reading. Using this free service, authors can make their results available to the community, in citable form, before we publish the edited article. This *Accepted Manuscript* will be replaced by the edited, formatted and paginated article as soon as this is available.

You can find more information about *Accepted Manuscripts* in the [Information for Authors](#).

Please note that technical editing may introduce minor changes to the text and/or graphics, which may alter content. The journal's standard [Terms & Conditions](#) and the [Ethical guidelines](#) still apply. In no event shall the Royal Society of Chemistry be held responsible for any errors or omissions in this *Accepted Manuscript* or any consequences arising from the use of any information it contains.

Cite this: DOI: 10.1039/c0xx00000x

www.rsc.org/xxxxxx

ARTICLE TYPE

## Study on Wear Behaviour and Wear Model of Nitrile Butadiene Rubber under Water Lubricated Conditions

Conglin Dong<sup>a, b</sup>, Chengqing Yuan<sup>\*a, b</sup>, Xiuqin Bai<sup>a, b</sup>, Xinping Yan<sup>a, b</sup>, Zhongxiao Peng<sup>c</sup>*Received (in XXX, XXX) Xth XXXXXXXXX 20XX, Accepted Xth XXXXXXXXX 20XX*

DOI: 10.1039/b000000x

Nitrile Butadiene Rubber (NBR) is widely used to make water-lubricated rubber stern tube bearings in the marine field. Its tribological properties, which significantly influence its reliability life, directly affect the safe navigation, covert performance and operating costs of a ship. This study aimed to investigate the tribological properties and wear model of NBR under water-lubricated conditions. A CBZ-1 tribo-tester was used to conduct sliding wear tests between NBR pins and 1Cr18Ni9Ti stainless steel discs under water-lubricated conditions. The surface morphologies of the worn NBR pins were examined using laser-interference profilometry and scanning electron microscopy. In addition, the friction coefficients, ageing times and wear rates were analysed and compared to study the tribological properties of NBR and to identify the factors that affect its wear mass loss. The results demonstrated that different ageing times, velocities and loads had a significant effect on the friction and wear properties of the NBR specimens. The ageing times positively correlated with the friction coefficients and the wear mass losses between the rubbing pairs. The anti-tear properties of NBR deteriorated when the material was aged at a high temperature for an extended period of time, which reduced its wear-resistance. The main wear mechanism between the rubbing pairs was severe adhesion tearing wear under the water-lubricated condition. A comprehensive empirical model for its wear rate estimation was established based on the wear and friction power. The model revealed the relationships between wear and velocity, as well as load and shore hardness. The result produced by the model was largely consistent with the experimental results. The knowledge gained in this study is anticipated to provide the theoretical data for a wear theory study of NBR and be useful for the optimisation of water-lubricated rubber stern tube bearings.

### 1. Introduction

The marine power system is a core component of ships, and stern tube bearings are an important constituent of the system. The concept of green ships and environmentally friendly vessels has become popular and has attracted the attention of researchers and end-users in recent years.<sup>1</sup> To relieve and eliminate the pollution of wasted lubrication oil, water-lubricated stern tube bearings have been proposed to replace oil-lubricated ones. Nitrile Butadiene Rubber (NBR) can absorb vibration and shows excellent chemical stability, water-resistance, wear-resistance and oil resistance properties.<sup>2</sup> Therefore, it is widely used to fabricate water-lubricated stern tube bearings in the marine field.<sup>3</sup>

However, the work environment of water-lubricated rubber stern tube bearings is extremely harsh, and their operation time is often very long. Thus, regular maintenance is normally required. Moreover, water is a poor lubricant for the bearings, which results in significant wear of the NBR stern tube bearings. The excessive wear of the NBR stern tube bearings reportedly is one of the most important reasons for the loss of their workability.<sup>4</sup> Recently, the excessive wear of these bearings resulted in the unscheduled lay off repair and maintenance of Coast Guard

ships.<sup>5</sup> Significant manpower and money is often spent on repairing and replacing worn parts. The excessive wear problem of NBR stern tube bearings has become increasingly prominent in recent years as the global competition and demand for production outputs and economic returns have increased.<sup>6</sup>

The tribological properties of NBR have not been well studied. Its basic mechanisms remain unexplored, though some relevant experimental observations have been presented. Based on the results of experimental studies by Champ and Southern, the physical process of rubber abrasion might be considered to be a crack-growth process.<sup>7,8</sup> The wear rate is a direct measure of a material wear property. If the wear trend of NBR is obtained using its wear rate, its remaining lifetime can then be predicted to ensure the safe navigation and reduce the operational costs of ships. Litwin and Mody noticed that the wear rate of composites is greater than the expected rate and that the relationship is nonlinear when the applied load is high.<sup>9,10</sup> The wear rate is also influenced by other factors, such as the hardness of the rubber and sliding speeds, etc. Zhang established an empirical wear loss formula based on the experimental results.<sup>11</sup> However, the equation formula only considered a single factor.

In reality, the wear of rubber is simultaneously affected by a number of factors, and their effects are not easy to evaluate

separately. Therefore, the objective of this work was to study the tribological properties of NBR and find the factors that affect its wear mass loss. An improved empirical model to estimate its wear mass loss rate was to be established. To achieve this objective, NBR specimens were tested against 1Cr18Ni9Ti stainless steel discs using a pin on a disc tribo-tester under water-lubricated conditions. The experimental apparatus and wear test details are explained in section 2. The results and discussions are presented in section 3 followed by the wear mass loss rate model and conclusions in sections 4 and 5, respectively. The ultimate goal was to improve the wear-resistance property of NBR and extend its service life in marine applications.

## 2. Experiments

### 2.1 Experimental Materials

The tests specimens used in this study were NBR pins (Fig. 1(a)) and 1Cr18Ni9Ti stainless steel discs (Fig. 1(b)). The diameter of the NBR pins was 10 mm, their height was 20 mm and their cross-sectional area ( $S$ ) was  $7.79 \times 10^{-5} \text{ m}^2$ . The surfaces of the

NBR specimens were polished with a grit polishing paper, and their surface roughness ( $S_a$ ) was measured to be  $1.51 \pm 0.5 \mu\text{m}$ . The counterpart was the 1Cr18Ni9Ti stainless steel disc with a 60 mm diameter. The thickness of the disc was 10 mm, and its surface roughness ( $S_a$ ) was  $0.65 \mu\text{m}$  as measured using a laser-interference profilometer (LI-3, China). The important mechanical properties of the NBR and 1Cr18Ni9Ti stainless steel samples are displayed in Tables 1 and 2, respectively.

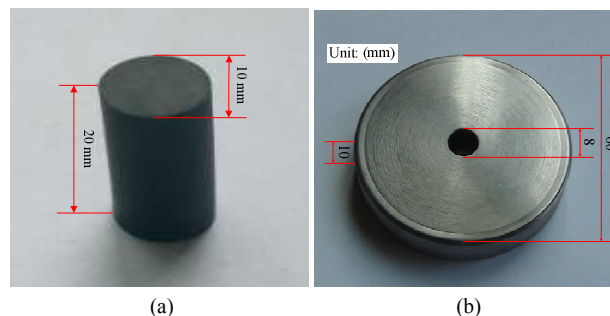


Fig. 1. (a) The NBR pin specimen; (b) The 1Cr18Ni9Ti stainless steel disc specimen

Table 1. Important mechanical properties of NBR without ageing and at a room temperature

Tensile strength (MPa)	Elongation at break (%)	Tensile set at break (%)	Volume change rate	Shore Hardness (A)	Poisson ratio	Young's modulus E (MPa)	Initial temperature of thermal decomposition (°C)
18~21	396	≤30	<5	63	0.49	5.83	233

Table 2. Important mechanical properties of 1Cr18Ni9Ti stainless steel

Hardness HRA* (MPa)	Young's modulus E (MPa)	Mass density $\rho$ (g/cm <sup>3</sup> )	Tensile strength (MPa)	Yield strength (MPa)	Elongation (%)
38	198	7.85	≥550	≥210	40

\* Rockwell A-Scale Hardness, Brale indenter, 60 kg load

The NBR pin samples were aged using a vacuum oven thermostat (SLH, China) to achieve different accelerated ageing conditions. The ageing temperature in the vacuum environment was set to 80°C to reduce the effect of temperature on the results.<sup>12</sup> The temperature fluctuating range was less than 1°C ( $\pm 0.5^\circ\text{C}$ ). A total of 60 pin samples were placed in the oven. Two specimens were removed every second day to measure their shore hardness; these samples were not placed back in the vacuum oven. The longest ageing time was 960 hrs (i.e. 40 days). The shore hardness is one of the most important parameters to characterise the mechanical properties of NBR. High ageing temperatures markedly affect this parameter.<sup>13</sup> This study selected the shore hardness of the NBR as the characteristic parameter. The behaviour of the shore hardness of the NBR pins for different accelerated ageing times is shown in Fig. 2. The shore hardness of NBR pins clearly positively correlated with the accelerated ageing times.

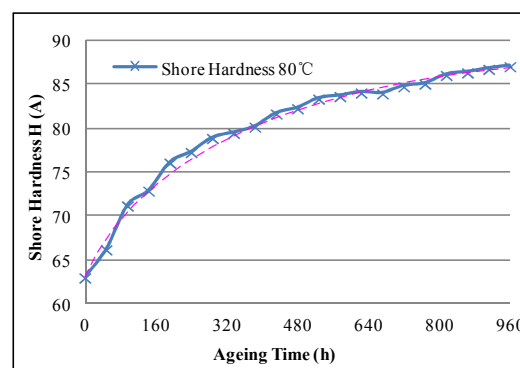


Fig. 2 Ageing time effects on the shore hardness of NBR

### 2.2 Experimental Apparatus and Sliding Wear Tests

All wear experiments were conducted using the CBZ-1 tribo-tester illustrated in Fig. 3. The sliding wear tests of the NBR pins against the 1Cr18Ni9Ti stainless steel discs were conducted under water-lubricated conditions. During the tests, the lower pin specimen made of NBR was submerged in distilled water and remained stationary, while the upper disc specimen of 1Cr18Ni9Ti stainless steel was sliding on the surface of a pin specimen with a rotational motion. Different loads, velocities and

ageing times were defined to study the tribological properties of NBR and find the factors that affect its wear mass loss.

The surface morphologies of the tested NBR pins were examined using a laser-interference profilometer and a scanning electron microscope (SU-70, Japan).

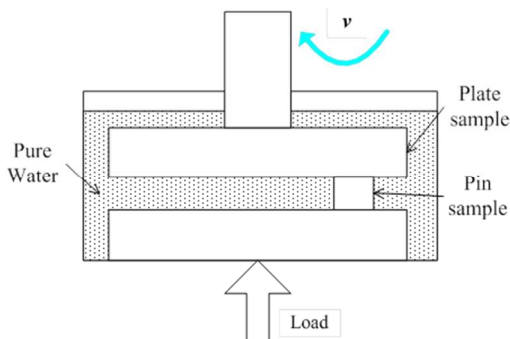


Fig. 3. A schematic sketch of the CBZ-1 tribo-tester used in this study

### 2.2.1 Sliding Wear Tests for Wear property Study Using Friction Coefficients

The un-aged NBR pins chosen to study effects of velocities and loads on the tribological properties of NBR. The rotational speed of the tribo-tester was set to 50, 150, 250, 350, 500 and 1000 rpm. The diameter of the sliding track was 42 mm. Therefore, the sliding velocities were 0.11, 0.33, 0.55, 0.77, 1.1 and 2.2 m/s. They were equivalent to 396, 1188, 1980, 2772, 3960 and 7920 m/h respectively. The nominal loads used were 7.9, 23.7, 39.5, 55.3, 71.1 and 86.9 N. Because the diameter of the NBR pins was 10 mm, the nominal pressures were 0.1, 0.3, 0.5, 0.7, 0.9 and 1.1 MPa. A total of 36 different sliding wear tests were conducted using the six speeds at 6 loading conditions.

The NBR pins that were aged for various accelerated ageing times were used to study the effects of ageing on the tribological properties of NBR. The different accelerated ageing times were 0, 120, 240, 360 and 480 hrs. The test nominal pressure was 0.5 MPa, and the rotational velocities of the tester were set to 0.11, 0.33, 0.55, 0.77, 1.1 and 2.2 m/s. A total of 30 different sliding wear tests were conducted using NBR pins with 5 different ageing times and the six speeds.

The duration of each test was 60 min. All sliding tests were repeated twice at the same condition to verify the repeatability of the results. The friction coefficients were measured every five seconds during the wear tests.

### 2.2.2 Sliding Wear Tests for Wear Mass Loss Analyses

The un-aged NBR samples were used to independently evaluate the load effects on the wear mass losses of NBR. To avoid the impact of velocities, the velocity was fixed at 0.77 m/s. The nominal pressures used were 0.1, 0.3, 0.5, 0.7, 0.9 and 1.1 MPa. A total of 6 different sliding wear tests were conducted using the one speed and the 6 loading conditions.

The un-aged NBR samples were used to examine velocity effects on the wear mass losses of NBR. The nominal pressure was set to a fixed value of 0.5 MPa. The velocities used were 0.11, 0.33, 0.55, 0.77, 1.1 and 2.2 m/s. A total of 6 different sliding wear tests were conducted using the 6 velocities and the one loading condition.

The NBR pins that were aged for various accelerated ageing times were used to study the effects of ageing durations on the

wear mass losses of NBR. The velocity and nominal pressure were set to fixed values, 0.77 m/s and 0.5 MPa, respectively. 50 different sliding wear tests were conducted on NBR pins with 5 different ageing times at the fixed loading and velocity conditions.

The duration of each test was 48 hrs to ensure the stability of the wear mass loss. The wear mass losses of the NBR pins were determined by measuring the weights before and after the tests. The tested specimens before weighing were ultrasonically cleaned in water and dried for 48 hrs in an oven at 50°C. The weight measurements were repeated four times for each specimen to ensure reproducible results using an analytical balance (MS205DU, Switzerland). The average friction power was the average friction work measured every hour after 48 hrs sliding wear tests. It is obtained as follows:

$$F = SP \quad (1)$$

$$\bar{f} = \bar{\mu}F = \bar{\mu}SP \quad (2)$$

$$L = vt \quad (3)$$

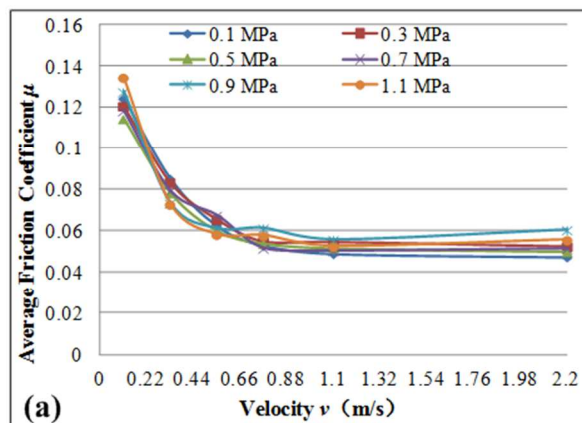
$$W = \frac{\bar{f}L}{t} = \frac{\bar{\mu}FL}{t} = \frac{\bar{\mu}SPL}{t} = v\bar{\mu}SP = Sv\bar{\mu}P \quad (4)$$

where  $W$  (J/h) is the average friction power,  $F$  (N) is the normal load,  $S$  is the contact surface area of the rubbing pairs, i.e. the cross-sectional area of the NBR pins,  $P$  (MPa) is the nominal pressure,  $\bar{f}$  (N) is the average frictional force,  $\bar{\mu}$  is the average friction coefficient between the rubbing pairs,  $L$  (m) is the sliding distance of the steel disc sliding on the surface of a pin specimen,  $t$  (h) is the sliding time and  $v$  (m/h) is the sliding velocity of the disc plate.

## 3. Results and Discussions

The tribological properties of the tested NBR specimens were investigated via comparison analyses of the friction coefficients, wear mass losses and worn surface topographies under different test conditions. The results are presented in the following sections, each of them focusing on a key tests variable or wear feature.

### 3.1 Analysis of Friction Coefficients



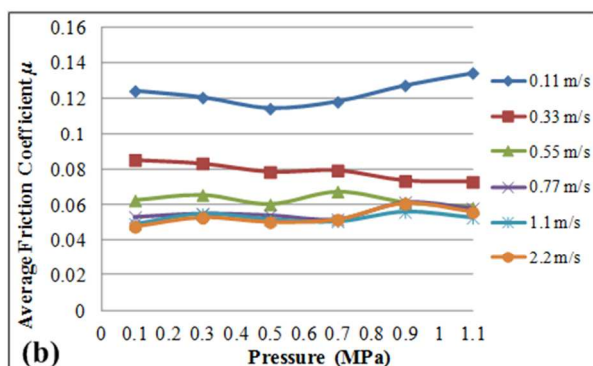


Fig. 4 (a) The velocity characteristic curves of the NBR pins without ageing; (b) The load characteristic curves of the NBR pins without ageing

The average friction coefficients between the NBR pins and 1Cr18Ni9Ti stainless steel disc rubbing pairs are shown in Fig. 4. Fig. 4(a) indicates that the average friction coefficients negatively correlated with the sliding velocities at the same nominal pressure conditions. When the velocities ranged from 0~0.66 m/s, the average friction coefficients decreased rapidly. They stabilised when the velocities exceeded 0.66 m/s. This effect may be due to the relatively obvious hydrodynamic lubrication between the NBR pins and 1Cr18Ni9Ti stainless steel disc rubbing pairs when the velocity was higher. This phenomenon could significantly improve the lubrication between rubbing pairs to decrease the friction coefficient. Some scholars have also reported the same phenomenon in their experiments.<sup>14-16</sup>

Fig. 4(b) clearly shows that the average friction coefficients changed marginally as the nominal pressures increased at the same velocity conditions. This finding may indicate that the loads had little effect on the friction coefficients between the rubbing pairs at the same condition.

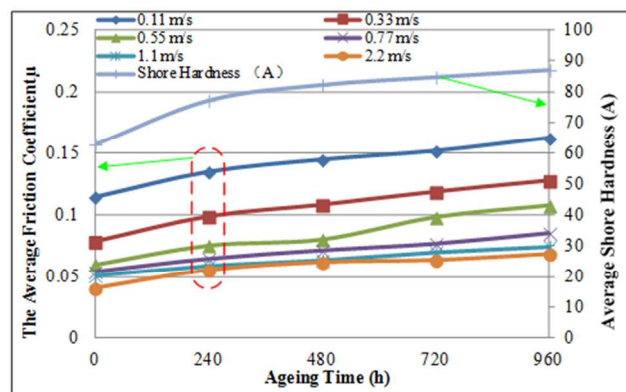


Fig. 5 Ageing effects on the friction coefficients of the NBR pins

The average friction coefficients for the NBR pins aged for various accelerated ageing times and 1Cr18Ni9Ti stainless steel disc rubbing pairs are presented in Fig. 5. The results showed that the accelerated ageing times affected the tribological properties of the NBR pins. In general, the average friction coefficients positively correlated with the accelerated ageing times for the same sliding velocity and nominal pressure conditions.

The sensitivity of the rubber material to temperatures was taken into consideration to explain the trend observed in Fig. 5 for the average friction coefficients as a function of the

accelerated ageing times. A high temperature significantly affects the rate of the chemical reactions of the material. This phenomenon will markedly change the cross-linked structure of the material. The mechanical properties of the material likely degrade in response to accelerated ageing at a high temperature for a long time. The shore hardness of the NBR was measured to study the ageing time effects. Figs. 2 and 5 show the behaviour of the shore hardness of NBR pins for different accelerated ageing times. The shore hardness positively correlated with the accelerated ageing times. Notably, the behaviours of the average friction coefficients between rubbing pairs were similar to those of the shore hardness as the in the accelerated ageing times increased. These trends are consistent with Roy's results.<sup>17</sup>

### 3.2 Analysis of Wear Mass Losses

The wear mass loss rates and average friction powers were measured to analyse the wear rates of the NBR pins. The wear mass loss rate was the average wear mass loss measured every hour after 48 hrs of sliding wear tests. The average friction power was the friction work measured every hour after 48 hrs of sliding wear tests.

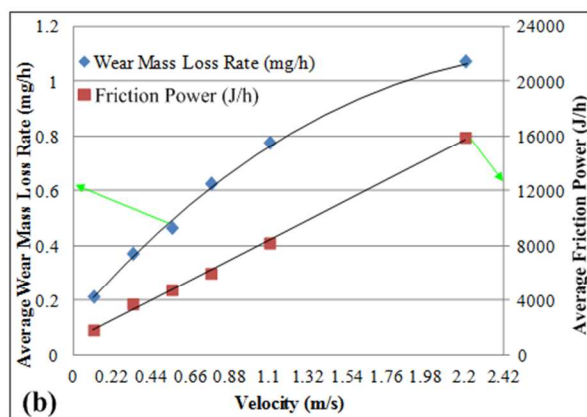
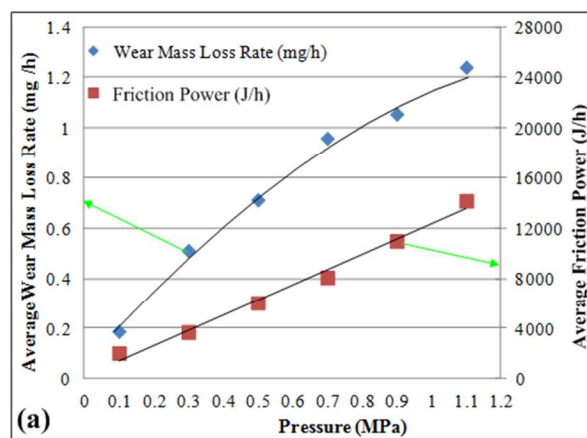


Fig. 6 (a) Nominal pressure effects on the wear mass loss rates and average friction powers of the NBR without accelerated ageing; (b) Speed effects on the wear mass loss rates and average friction powers of the NBR without accelerated ageing

The changes in the wear mass loss rates and average friction powers of the un-aged NBR at nominal pressures are shown in Fig. 6(a). The average wear mass loss rates of NBR positively correlated with the nominal pressure. The average friction powers

linearly increased as the pressure increased. The pressure clearly positively correlated with the friction powers between the rubbing pairs. As a result, the NBR was more easily worn out in the sliding wear process.

As shown in Fig. 6(b), the average wear mass loss rates of the un-aged NBR positively correlated with the sliding velocities for the same nominal pressure tested conditions. The average friction powers showed mostly linear increases.

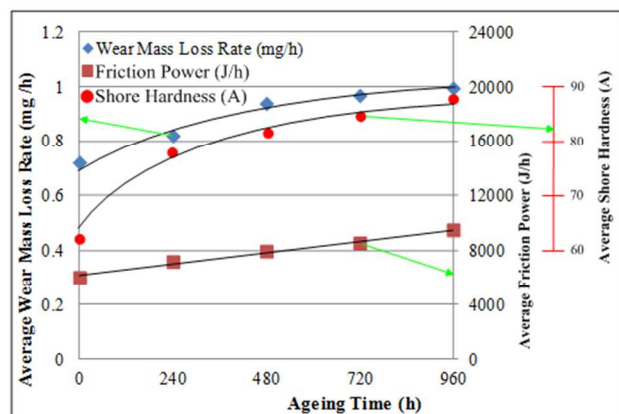


Fig. 7 The behaviour of the wear mass loss rates and friction powers of the NBR pins for different accelerated ageing times

The behaviours of the wear mass loss rates and friction powers of the NBR pins aged for various accelerated ageing times are shown in Fig. 7. The wear mass loss rates of the aged NBR pins clearly positively correlated with the ageing times for the same nominal pressure and velocity conditions. When the ageing time exceeded 720 hrs, the slope of the curve decreased, which indicated that the wear rates slowed. However, the average friction powers linearly increased. As presented in section 3.1, this behaviour may arise because the ageing processes promoted the degradation of the anti-fatigue and anti-tear properties of the NBR, resulting in a higher wear rate than that of the pin specimens not subjected to the ageing processes at the same nominal pressure and velocity conditions.<sup>18</sup> This notion can be indirectly proven by the shore hardness values of NBR pins for different accelerate ageing times. The shore hardness of NBR pins positively correlated with the accelerated ageing times, as shown in Figs. 2 and 7.

Figs. 6 and 7 show that both the wear mass loss rates and the friction powers increased with the pressure, velocity and ageing time. These two rates were hypothesised to be related. This paper will attempt to reveal this relationship section 4.

### 3.3 Understanding of Wear Mechanisms

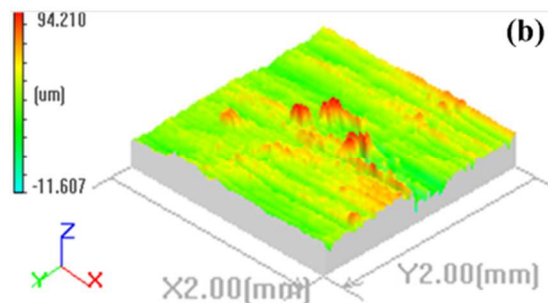
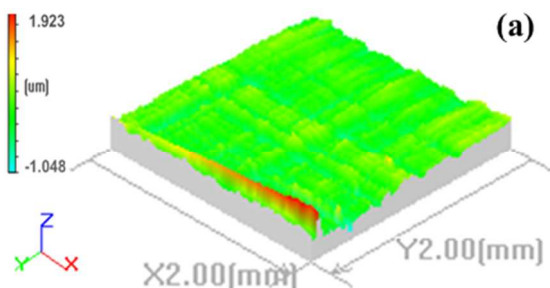


Fig. 8 The untested (a) and worn surface topographies before test; (b) of the tested NBR pins after test

The examinations of the worn surfaces of the rubbing pairs after the tests revealed that the tested surfaces of the disc experienced minimal wear. In contrast, significant wear occurred on the surfaces of the NBR pins. The worn surface topographies of the NBR pins were closely examined using a laser-interference profilometer.<sup>19,20</sup> Fig. 8 shows the surface topographies of one untested and tested NBR pins. Obvious furrows and material accumulation on the worn surface of the untested NBR are absent in Fig. 8(a). However, many furrows and deformed NBR asperities are visible on the worn surfaces of the NBR pins in Fig. 8(b). The analyses and these phenomena suggest that the material on the wear surface of NBR pins experienced stress due to the friction and wear between the rubbing pairs in the sliding wear progress. This stress will result in the plastic yield deformation of the NBR material. As a result, the NBR material yielded plastic deformation will accumulate on the worn surface and form additional NBR asperities.

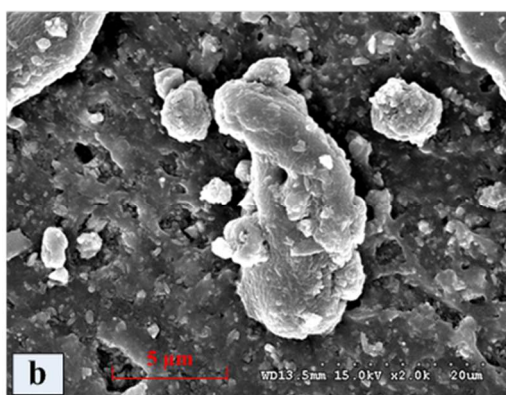
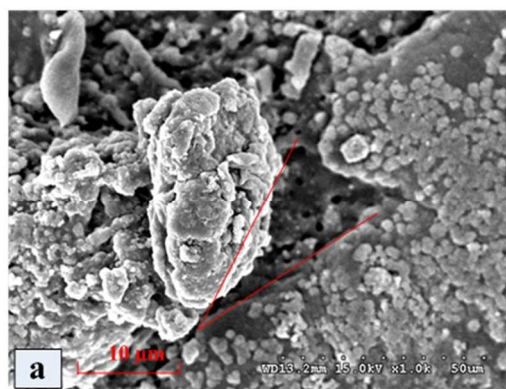


Fig. 9 The SEM images of the tested NBR pins. (a) a curly NBR asperity on the worn surface; (b) a wear particle on the worn surface.

To study the wear characteristics and mechanisms, the worn surface topographies of the NBR pins were examined using scanning electron microscopy (SEM). As shown in Fig. 9(a), a curly NBR asperity was evident on the worn surface. A tearing phenomenon was apparent at the contact position between the NBR asperity and the worn surface. Fig. 9(b) shows that part of the material was peeled off from the worn surface to form a wear particle.

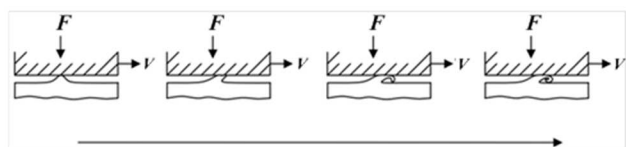


Fig. 10 The formation of the curly NBR asperities

The above analyses indicate that the friction and wear characteristics between the NBR pins and 1Cr18Ni9Ti stainless steel disc rubbing pairs are very particular. The NBR asperities on the surface were stretched or deformed along the sliding direction of the upper disc. When the anti-fatigue and anti-tear properties of NBR pins are not sufficient to resist the combined actions of the adhesion and tensile stress, cracks form on the severely stretched NBR surfaces in the direction perpendicular to the stretching direction. At the beginning, the expansion of the cracks will not cause the deformed NBR asperities to peel off. Instead, this expansion often causes the NBR asperities on the worn surface of the NBR pins to be gradually torn along the sliding direction of the upper disc. The deformed NBR asperities will be further stretched into a long and curved feature, as shown in Fig. 10. The curly NBR asperities are in a stressed state. When the anti-tear property is insufficient to resist the combined actions of the adhesion and tensile stress, part of the curly NBR asperities will be peeled off from the surface and wear particles will be generated. Therefore, the main wear mechanism between the NBR pins and 1Cr18Ni9Ti stainless steel discs rubbing pairs is severe adhesion tearing wear under the water-lubricated condition.

## 4. Development of a Wear Rate Model

### 4.1 Theory of Wear Rate

Uchiyama proposed the wear energy theory.<sup>21</sup> He considers that the total friction work,  $E_f$ , required to transform a small rubber asperity into a wear particle can be described using Eq. 5:

$$E_f = E_i + E_e \quad (5)$$

where  $E_i$  is the crack-growth energy, and  $E_e$  is the rupture energy of the curly rubber asperity.

Eq. 5 provides two inferences: the number of the rubber wear particles positively correlates with the friction work at the same condition. Furthermore, less energy is required to make the rubber asperity into the wear particle if the mechanical properties of rubber degrade due to other influences, such as accelerated ageing; thus, the number of the wear particles will increase per unit friction work.

However, the theoretical relationship between the wear mass loss rates and the friction powers is not easily determined. Zhang

and Liang experimentally determined that the friction work significantly affects the wear mass loss rates for rubber materials.<sup>22-24</sup>

The results and phenomena mentioned above suggest that the wear mass loss rates of NBR are in accordance with a power function for the increase in the friction powers, and the wear mass loss rate,  $A$ , can be estimated from the following equation:

$$A = kW^n \quad (6)$$

where  $A$  is the wear mass loss rate of NBR pins in mg/h.  $k$  and  $n$  are the constants accounting for the properties of the materials and shape of the pins in this test, respectively; they are experimentally determined.

Based on Eqs. 4 and 6,  $A$  is described by the following equation:

$$A = k\bar{\mu}^n S^n P^n v^n \quad (7)$$

The friction coefficient between the rubbing pairs is apparently very important to the wear mass loss rates of NBR. In general, the friction coefficients are determined during the tests. Based on the experimental results mentioned above and previous studies, the friction coefficient between the rubber and smooth metal surface under the water-lubricated conditions is related to the velocity, load and the ageing degree of the rubber.<sup>25,26</sup> Eq. 8 describes the hypothesised approximate relationship between these parameters:

$$\bar{\mu} = av^b H^c F^d = av^b H^c S^d P^d \quad (8)$$

where  $a$  is the constant that accounts for the properties of the materials;  $b$ ,  $c$  and  $d$  are the constants that account for the shape of the pins.  $H$  (A) is the characteristic parameter that characterises the mechanical properties of NBR. This study selected the shore hardness of the NBR as the characteristic parameter. Hence,

$$A = ka^n v^{nb} H^{nc} S^{nd} P^{nd} S^n P^n v^n = ka^n S^{nd+n} H^{nc} P^{nd+n} v^{nb+n} \quad (9)$$

$n$ ,  $k$ ,  $a$  and  $d$  are the constants;  $S$  is the cross-sectional area of the NBR pins. For the ease of calculation,  $ka^n S^{nd+n}$  is replaced by the constant  $q$ ,  $nc$  is replaced by the constant  $\alpha$ ,  $(nd+n)$  is replaced by the constant  $\beta$  and  $(nb+n)$  is replaced by the constant  $\gamma$ . Therefore,

$$A = qH^\alpha P^\beta v^\gamma \quad (10)$$

### 4.2 Effects of Pressures on Wear Rates

To investigate the effect of the pressure index constant  $\beta$  on the wear mass loss rates of NBR, the un-aged NBR pins were tested as described in section 2. To avoid the impact of velocity, the velocity was set to a fixed value, i.e. 2772 m/h. The results are shown in Table 3.

**Table 3.** The worn mass loss rates of NBR pins without ageing for different nominal pressures at the same velocity condition (2772 m/h)

Nominal Pressures (MPa)	0.1	0.3	0.5	0.7	0.9	1.1
Wear Mass Loss Rates (mg/h)	0.185	0.509	0.71	0.958	1.054	1.239

Because  $H^\alpha$  and  $v^\gamma$  were constant,  $qH^\alpha v^\gamma$  could be replaced by

the constant  $q_1$ . Therefore, the following empirical formula could describe the relationship between the nominal pressures and the wear mass loss rate,  $A$ .

$$A = q_1 P^\beta \quad (11)$$

A regression analysis using Matlab was carried out on the data in Table 3 to obtain the constants  $\beta$  and  $q_1$ . The value of  $q_1$  was 1.205, and the value of  $\beta$  was 0.7876.

### 4.3 Effects of Velocities on Wear Rates

To determine the effect of the velocity index constant  $\gamma$  on the wear mass loss rates of NBR, the un-aged NBR pins were used in the wear tests detailed in section 2. To avoid the impact of pressure, a fixed nominal pressure was defined at 0.5 MPa. The relationship between the wear rate and the velocity is illustrated in Table 4.

**Table 4** The worn mass loss rates of un-aged NBR pins for different velocities at the same nominal pressure condition (0.5 MPa)

Velocities (m/h)	396	1188	1980	2772	3960	7920
Wear Mass Loss Rates (mg/h)	0.215	0.373	0.467	0.627	0.777	1.075

Because  $H^\alpha$  and  $P^\beta$  were constant,  $qH^\alpha P^\beta$  could be replaced by the constant  $q_2$ . Therefore, the follow empirical formula could describe the relationship between the velocity and the wear mass loss rate,  $A$ .

$$A = q_2 v^\gamma \quad (12)$$

A regression analysis of the data in Table 4 was conducted to obtain the constants  $\gamma$  and  $q_2$ . The value of  $q_2$  was 0.0078, and the value of  $\gamma$  was 0.5499.

### 4.4 Effects of Ageing times on Wear Rates

The NBR pins subjected to accelerated ageing were tested to determine the effect of the ageing index constant  $\alpha$  on the wear mass loss rates of NBR. To avoid the impact of pressure and velocity, the pressure was fixed at 0.5 MPa and the velocity was fixed at 2772 m/h. The wear rate results are shown in Table 5

**Table 5.** The worn mass loss rates of aged NBR pins for different shore hardness values at the same nominal pressure and velocity condition (0.5 MPa, 2772 m/h)

Shore Hardness (A)	63 (Without ageing)	77.3 (Ageing 240 hrs)	82.3 (Ageing 480 hrs)	84.8 (Ageing 720 hrs)	87.1 (Ageing 960 hrs)
Wear Mass Loss Rates (mg/h)	0.719	0.819	0.938	0.967	0.994

Because  $v^\gamma$  and  $P^\beta$  were unchanged,  $q v^\gamma P^\beta$  could be replaced by the constant  $q_3$ . Therefore, the following empirical formula could describe the relationship between the shore hardness and the wear mass loss rate,  $A$ .

$$A = q_3 H^\alpha \quad (13)$$

A regression analysis of the data in Table 5 was conducted using Matlab to obtain the constants  $\alpha$  and  $q_3$ . The value of  $q_3$  was 0.0106, and the value of  $\alpha$  was 1.0133.

### 4.5 Comprehensive Empirical Wear Rate Formula

As indicated above,  $q_1 = qH^\alpha v^\gamma$ ,  $q_2 = qH^\alpha P^\beta$  and  $q_3 = qv^\gamma P^\beta$ . The values of  $q_1$ ,  $q_2$ ,  $q_3$ ,  $H$ ,  $P$ ,  $v$ ,  $\alpha$ ,  $\beta$  and  $\gamma$  were obtained. The three values of  $q$  were  $2.315 \times 10^{-4}$ ,  $2.027 \times 10^{-4}$  and  $2.34 \times 10^{-4}$ . The average of these values,  $2.227 \times 10^{-4}$ , was chosen as the constant  $q$ . Hence, the comprehensive empirical formula, which describes the wear mass loss rate as a function of the shore hardness, velocity and the load, was obtained:

$$A = 2.227 \times 10^{-4} H^{1.0133} P^{0.7876} v^{0.5499} \quad (14)$$

The wear mass loss rates of NBR pins at the other tests conditions were obtained based on the comprehensive empirical wear mass loss rate formula.

To verify the accuracy of the formula, the other conditions were tested using the tribo-tester detailed in section 2.2.2. The un-aged NBR pins were used in the wear tests. The velocity and nominal pressure were set to 1188 m/h and 0.3 MPa, respectively. The wear rates estimated using the above formula were compared with the experiential results. The relative error ( $e$ ) was calculated using the following formula (15).

$$e = \frac{|\bar{A} - A|}{A} \times 100\% \quad (15)$$

where  $\bar{A}$  (mg/h) is the wear mass loss rates obtained using experiments, and  $A$  (mg/h) is the wear mass loss rates obtained using empirical formula. The errors between these two rates are shown in Tables 5-6.

**Table 6.** The errors between the results predicted and experiential results; NBR pins without ageing with different nominal pressures and under the same velocity conditions (63A, 1188 m/h)

Nominal Pressures (MPa)	0.1	0.3	0.5	0.7	0.9	1.1
$\bar{A}$ (mg/h)	0.125	0.301	0.4	0.598	0.654	0.859
$A$ (mg/h)	0.119	0.282	0.421	0.549	0.669	0.784
$e$	4.8%	6.3%	5.3%	8.2%	2.3%	8.7%

**Table 7.** The errors between the results predicted and experiential results; NBR pins without ageing with different velocities and under the same nominal pressure conditions (63A, 0.3 MPa)

Velocities (m/h)	396	1188	1980	2772	3960	7920
$\bar{A}$ (mg/h)	0.145	0.273	0.407	0.427	0.537	0.708
$A$ (mg/h)	0.154	0.282	0.373	0.449	0.546	0.799
$e$	6.2%	3.3%	8.4%	5.2%	1.7%	12.9%

As shown in Tables 6-7, the largest error was 12.9%; the others errors were less than 10%. Generally speaking, the errors were in line with the expectations. They could be accepted in engineering practice. These errors indicate that the comprehensive empirical wear mass loss rate formula is suitable for predicting the wear mass loss rates of NBR pins tested against 1Cr18Ni9Ti stainless steel under water-lubricated conditions. This applicability of this formula to other test conditions should be further examined.

## 5. Conclusions

The sliding wear tests of NBR pins against 1Cr18Ni9Ti stainless steel were conducted using a tribo-tester under water-lubricated conditions. The tribological properties of the tested NBR specimens were investigated by comparing the friction coefficients, wear mass losses and worn surface topographies for different test conditions. The loads, ageing time and velocities were found to significantly affect the wear mass loss rates of the NBR. The following conclusions were drawn as the outcomes of this study:

- (a) High-temperature accelerated ageing significantly affected the friction and wear properties of the NBR specimens. The friction coefficients between the rubbing pairs and the wear mass losses of the NBR positively correlated with the ageing times.
- (b) The main wear mechanism between the NBR pins and the 1Cr18Ni9Ti stainless steel rubbing pairs is severe adhesion tearing wear under the water-lubricated condition.
- (c) A comprehensive empirical wear mass loss rate formula was established to describe the wear rule of the NBR. Overall, the wear rates estimated by the formula are comparable with the experimental results.
- (d) The knowledge gained in this study will provide the theoretical data for studying the wear theory of NBR and is useful for the optimisation of water-lubricated rubber stern tube bearings.

## Acknowledgments

This study was supported by the State Key Program of National Natural Science of China (51139005), the Program for New Century Excellent Talents in University (NCET-12-0910), the Fundamental Research Funds for the Central Universities (2012-II-018 and 2012-YB-13) and the Program of Introducing Talents of Discipline to Universities (B08031).

## Notes and references

- <sup>a</sup> School of Energy and Power Engineering, Wuhan University of Technology, Wuhan 430063, P.R. China. Fax: +86-27-86549879; Tel: +86-27-86554969; E-mail: ycq@whut.edu.cn
- <sup>b</sup> Key Laboratory of Marine Power Engineering & Technology (Ministry of Transport), Wuhan University of Technology, Wuhan 430063, P.R. China. Fax: +86-27-86549879; Tel: +86-27-86554969; E-mail: ycq@whut.edu.cn
- <sup>c</sup> School of Mechanical and Manufacturing Engineering, The University of New South Wales, Sydney 2052, Australia. E-mail: z.peng@unsw.edu.au
- 1 X. Yan, C Yuan, X Zhou and X Bai, *Advanced Tribology*, 2010, 957.
  - 2 L. Liang, S Zhao, L Zhu and C. Yao, *China Synthetic Rubber Industry*, 2012, 35, 17.
  - 3 C. Dong, C. Yuan, Z. Liu and X. Yan, *Advanced Shipping and Ocean Engineering*, 2013, 2, 27.
  - 4 R. Vie, L. Hampson, *The Institute of Marine Engineers*, 2000, 112, 11.
  - 5 H. Hirani, M. Verma, *Tribology International*, 2009, 42, 378.
  - 6 F. Andritsos, H. Cozijn, *ASME 2011 30th International Conference on Ocean*, 2011, 2, 73.
  - 7 D. Champ, E. Southern and A. Thomas, *In Advances in Polymer Friction and Wear*, Plenum Press, New York, 1974.
  - 8 E. Southern, A. Thomas, *Rubber Chemicl Technology*, 1979, 52, 1008.
  - 9 W. Litwin, *Tribology Transactions*, 2011, 54, 351.

- 10 P. Mody, T Chou and K. Friedrich, *Journal of Materials Science*, 1988, 23, 4319.
- 11 W. Zhang, *Journal of Materials Science*, 1995, 30, 4561.
- 12 E. Bystritskaya, A Pomerantsev and O. Rodionova, *Polymer Testing*, 2000, 19, 221.
- 13 V. Subrahmanian, S. Ganapathy, *Journal of Applied Polymer Science*, 2000, 78, 2500.
- 14 R. Daugherty, N. Sides, *ASLE transactions*, 1981, 24, 293.
- 15 K. Tanaka, *Wear*, 1982, 75, 183.
- 16 J. Mens, *Wear*, 1991, 149, 255.
- 17 L. Roy, J. Orndorff, *Journal of Tribology*, 2000, 122, 367.
- 18 B. Likozar, Z. Major, *Applied Surface Science*, 2010, 257, 565.
- 19 C. Yuan, J. Li, X. Yan and Z. Peng, *Wear*, 2003, 255, 315.
- 20 C. Yuan, Z. Peng, X. Zhou and X. Yan, *Wear*, 2005, 259, 512.
- 21 Y. Uchiyama, Y. Ishino, *Wear*, 1992, 158, 141.
- 22 S. Zhang, Z. Yang, *Tribology International*, 1997, 30, 839.
- 23 S. Zhang, *Rubber Chemical Technology*, 1984, 57, 769.
- 24 H. Liang, Y. Fukahori and A. Thomas, *Wear*, 2009, 266, 288.
- 25 H. Qin, X. Zhou, C. Xu, H. Wang and Z. Liu, *The Open Mechanical Engineering Journal*, 2012, 6, 133.
- 26 A. Moshkovich, V. Perfilyev and I. Lapsker, *Tribology Letters*, 2011, 42, 89-98.